Simulating electromagnetic response in coupled metallic nanoparticles for nanoscale optical microscopy and spectroscopy: nanorod-end effects

Garnett W. Bryant[a], Isabel Romero[b], F. Javier García de Abajo[b,c], Javier Aizpurua*[b]
[a]National Institute of Standards and Technology, 100 Bureau Drive, Gaithersburg, MD, USA 20899
[b]Donostia International Physics Center, P. Manuel Lardizabal 4, San Sebastián 20018, Spain
[c]Instituto de Optica, CSIC, C/ Serrano 121, Madrid 28006, Spain

ABSTRACT

Collective oscillations of valence electrons in metallic materials determine their optical response. The energy and strength of these surface oscillations are a function of the shape, size and coupling of the nanoparticles. With the use of a boundary element method (BEM), we solve Maxwell's equations to calculate light scattering and surface modes in nanorods that are commonly used as hosts and/or samples in different field-enhanced scanning-probe microscopies and spectroscopies. We calculate the near-field and far-field response of nanorods and show that different geometrical terminations of the rods give different optical response in the far field for short rod lengths. For longer lengths, the response of rods with different terminations becomes more similar. The near field features of the ends become most evident close to the rod structural features that define the end capping. We identify four regimes for the separation between nanorod pairs that provide different coupling between nanorods. We also show that the size dependence of the nanorod response is characterized by a rod radius that gives a minimum wavelength for the dipolar response. For thicker and thinner rods, the response redshifts.

Keywords: Surface plasmons, Metallic nanoparticles, Nanorods, Nanowires, Surface enhanced spectroscopy, SERS

1. INTRODUCTION

Metallic nanostructures have become the subject of intense research recently, because of their use as electromagnetic field enhancers and transmitters on the nanoscale, and their applications in nanoscale optical metrology. Resonant optical antennas in the visible for efficient continuum light emission (1), integrated nanoantennas for single photon detection (2), use in hybrid nano-conjugates for enhanced light emission (3), nanoprobes for diagnosis and selective detection (4), near-field optical microscopy of nanoscale objects (5), and the detection of electromagnetic energy transport in nanoarrays (6) are some of the most challenging applications that make use of the resonances of metallic nanostructures. Moreover, a variety of metallic nanoparticles have been used in nanoscale microscopy and spectroscopy to enhance light scattering and near-field signals. The optical response of particles and coupled systems such as nanospheres (7), nanodisks (8), nanorings (9), nanorods (10,11), nanoshells (12,13), have been systematically studied both theoretically and experimentally during recent years because their optical response and be controlled and tuned via size and shape. Usually, the field enhancement at a selected wavelength is achieved from the control of strong intra- and/or inter-coupling between resonances on individual/or coupled metallic nanoparticles. The interest in nanorods as metallic hosts for field-enhanced microscopy and spectroscopy is not restricted to the optical range of the spectrum. Promising studies on the infrared response in micrometric nanorods (14) make these entities appropriate candidates for infrared spectroscopy of molecules of biological interest by means of surface infrared absorption (SEIRA).

In this paper we present a detailed study of the optical resonances in single and coupled nanorods, and we show how the size, shape (i.e. the termination of the rods) and coupling affects these resonances. We focus on gold nanorods because their response can be significantly tuned via the control of size, shape and coupling. We show that nanorod resonances differ from those in antenna theory due to the finite conductivity of gold. We determine how the near and far field depend on the detail of the particle end geometry and establish that this effect is most important for short rods. Finally,

*aizpurua@ehu.es; phone +34 943 01-5624; fax +34 943 01-5600; http://dipc.ehu.es

Plasmonics: Metallic Nanostructures and their Optical Properties IV, edited by Mark I. Stockman,
Proc. of SPIE Vol. 6323, 632313, (2006) · 0277-786X/06/$15 · doi: 10.1117/12.680701

we study the effect of the rod size (width) on its resonances. As we will show, both size and geometry significantly influence the near and far field response of metallic nanorods.

2. BOUNDARY ELEMENT METHOD FOR OPTICAL RESPONSE

Analytical solutions of both Poisson's and Maxwell's equations for simple geometries can be developed with the use of a more or less complicated sets of coordinates and expansions. As the geometry of a particle becomes more complicated, or there is complex coupling between several metallic particles, the light scattering can be determined with numerical calculations that match the boundary conditions over the interfaces separating the different media. We use a Boundary Element Method (BEM) to solve Maxwell's equations in the presence of inhomogeneous media (15-17). A self-consistent set of induced surface charge densities and currents are determined for the different interfaces. This set of charges and currents satisfies the boundary conditions and couples to the external field giving rise to the optical response of the inhomogeneous geometry. The method has been successfully applied to deal with the response of nanorings, nanodisks, and nanorods, with strong sensitivity to geometry, where standard analytical methods where difficult to apply. Intuitively, in the non-retarded approximation, the induced charges $\sigma(\mathbf{s},\omega)$ at the interface between medium A and B, characterized by their dielectric constants $\varepsilon_A(\omega)$ and $\varepsilon_B(\omega)$ fulfills:

$$\Lambda(\omega)\sigma(\boldsymbol{s},\omega) = \boldsymbol{n}(\boldsymbol{s})\cdot\nabla\phi_{ext}(\boldsymbol{s},\omega) - \int \frac{\boldsymbol{n}(\boldsymbol{s})\cdot(\boldsymbol{s}'-\boldsymbol{s})}{|\boldsymbol{s}'-\boldsymbol{s}|^3}\sigma(\boldsymbol{s}',\omega)d^2\boldsymbol{s}' \tag{1}$$

with

$$\Lambda(\omega) = 2\pi\frac{\varepsilon_A+\varepsilon_B}{\varepsilon_B-\varepsilon_A} \tag{2}$$

and $\mathbf{n}(\mathbf{s})$ the unit vector normal to the interface at each surface point $\mathbf{s}$. The induced surface charges give rise to the near and far field response. A similar set of self-consistent equations, involving currents in addition to the induced charges, accounts for the solution of Maxwell's equations, thereby including retardation in the response (16,17).

As an example of the method, we show the induced surface charge of the first surface mode and the near-field of a gold nanorod antenna with hemispherical ends where the position of the resonance depends on the length and diameter of the rod forming the antenna.

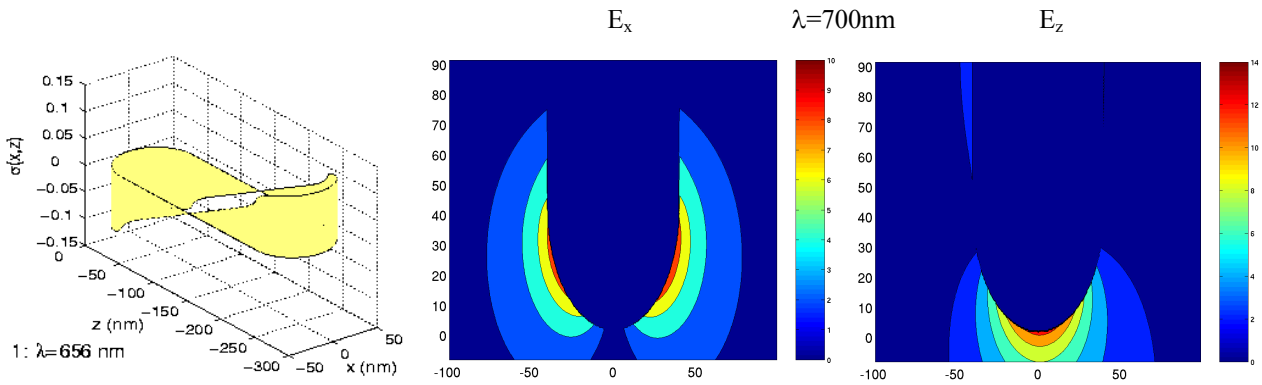

Fig. 1. (Left) Dipolar mode of a gold nanoantenna as obtained from the solution of Poisson's equation with the BEM. (Middle and right) Near field distribution at one end of a 200 nm long gold nanoantenna with the incoming light polarized along rod axis.The nearfield polarized parallel to the direction of incidence (middle) and the near field polarized along the rod axis (right) are shown.

The dipolar mode displayed on the left hand side of Fig. 1 is responsible for the main response of a nanorod to the incoming light. The near field distribution is enhanced near the edge of the nanorod giving a field enhancement of about 14 times along the rod axis. The wavelength of this first resonance does not appear exactly at twice the rod length, as in standard antenna theory. The resonance is at longer wavelength due to how the induced charge accumulates at the ends of the rod.

3. COUPLED NANORODS

An useful configuration that establishes the capacity for resonance tunning and near-field enhancement arises when two nanorods are coupled together across a gap between the ends, forming a nanocavity where the induced charge density can pile up. Schematically, the surface charge pattern follows that of two aligned dipoles with a concentrated induced charge at the gap, with thecompensating charge spread over the rest of each nanorod to insure that charge neutrality on each rod is maintained. The length and radius of the rods determine how much this charge can pile up. We show schematically the pattern of charge polarization for these structures on the left hand side of Fig. 2.

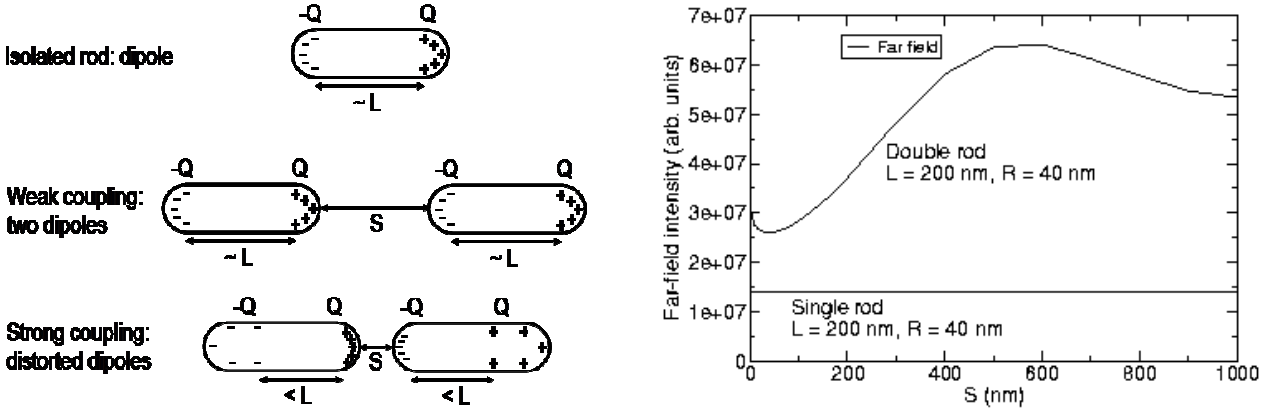

Fig. 2. (Left) Scheme of the charge polarization for an isolated nanorod versus weakly coupled nanorods for large separation (S) and strongly coupled nanorods for small separation distance. (Right) Far field intensity for a 200 nm long, 40 nm wide double rod as a function of separation distance S, compared to the far field of an isolated rod of the same size.

Fig. 2 shows how the charge distribution piles up at the cavity formed by the double nanorod when the separation distance S is decreased. On the right hand side of Fig. 2 we observe how the far field intensity for transmission of a polarized wave is enhanced for a double nanorod as a result of the interrod coupling. For very widely separated rods, the far-field intensity should be 4 times the intensity of a single rod. That limit is approached for large S with oscillations about this limit that are due to interference. At smaller S, the far-field response decreases below this limit. In this regime, the induced charge distribution on each rod is distorted by the interrod coupling. The charge at the outside ends of the dimer is pulled closer to gap, reducing the effective dipole moment of the pair and leading to the reduce far-field intensity. At even smaller S, the far-field intensity grows again, due the strong charge localization at the gap. This is the regime of strong near-field enhancement. Finally, for very small S, there is a fourth regime, not visible here, associated with singular redshifts of the resonance wavelengths with decreasing S and suppression of the response because the charge across the gap is so strongly coupled that all other oscillation is inhibited.

4. END EFFECTS

We present in this section the effects of different geometrical terminations of the rods on the light scattering. Three terminations are considered to account for the different possible curvatures at the ends: hemispherical (H), flat (F) and concave (C) with inner radius D, which is chosen smaller than R to avoid singularities due to sharp edges:

Fig. 3. Scheme of the different terminations considered for nanorods: hemispherical (H), flat (F), and concave (C) ends.

4.1 Far-field response

We first identify how the far-field response differs for rods with different terminations. In Fig. 4, we show spectra of the transmitted intensity for incident light polarized along the rod axis. Long and short rods and different terminations are considered: both ends hemispherical (H-H), both ends flat (F-F), both ends concave (C-C), and different combinations of the terminations (FH, CH, CF). For short rods (L=100nm), the hemispherical and flat ends have similar resonances, although rods with flat ends provide lower enhancement due to the shorter effective length of the nanorod. The concave ends have sharper resonances associated with modes localized at the tips of the concave ends. For longer rods (L=200nm), the edge effects become less important, and the far field radiation is governed by the rod as a whole, rather than the detail of the edges (see Fig. 4 (right)). Concave ends still show sharper resonances because of the sharper tips.

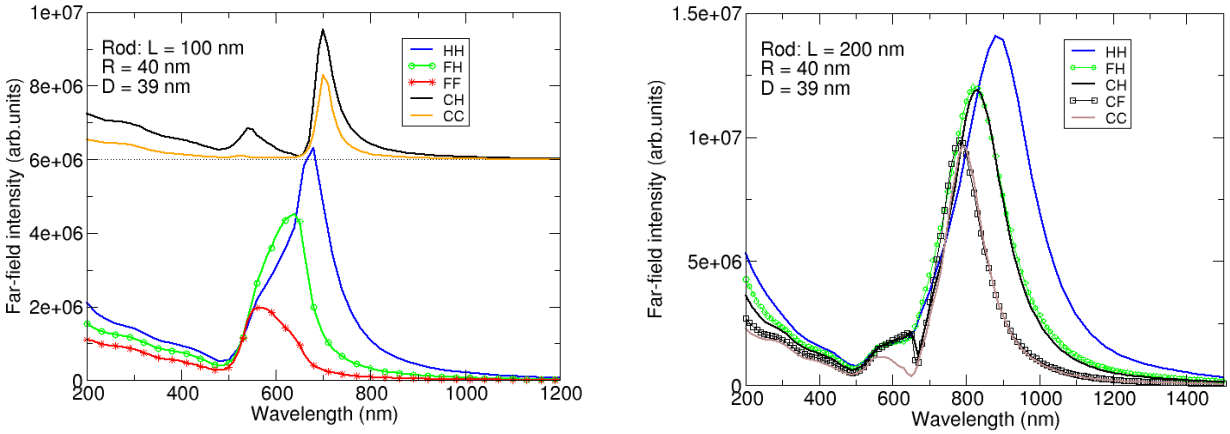

Fig. 4. (Left) Far-field intensity transmitted for 100 nm long rods showing different types of ends: hemispherical (HH), flat (FF), concave (CC), and combined ends (FH) and (CH). (Right) Far field intensity for a 200 nm long, 40 nm radius rod. Longer rods show less spectral dependence on the geometry of the ends.

4.2 Near-field response

The near-field spectrum of the rods considered in the previous section show features similar to those for the far field with sharper resonances for rods with concave ends. The near-field distribution around the edges shows different patterns for different terminations which might be important for hot site location in surface enhanced spectroscopy. Hemispherical and flat ends show enhancements of the order of 10-12 times in amplitude, whereas enhancement for concave ends can be up to 20 times for particular locations near the edge tips. We plot the near field distribution at resonant wavelength for the flat (F) and concave (C) cases for the field perpendicular and parallel to the rod in Fig 5.

The main difference between the hemispherical end and the flat end is that the charge piles up at the corners of the edge (see Fig. 5 top). For a rod with concave ends, the strong local character of the oscillation along the concave protrusion at the end is apparent.

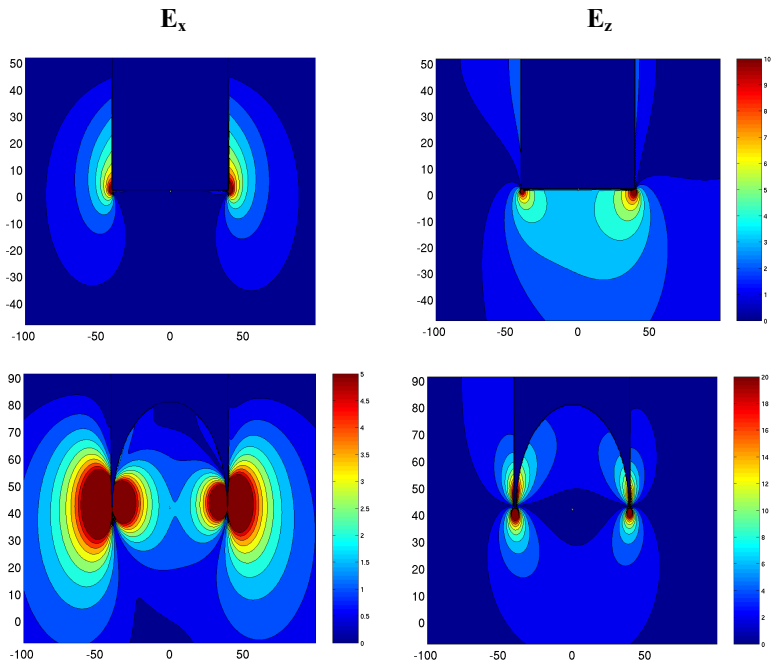

Fig. 5. (Top) Near field distribution for a rod with flat ends. (Bottom) Near field distribution of a rod with concave ends at resonance. In both cases, graphs on the left show electric field in x- direction, and graphs on the right show the electric field along the z direction.

4.3 Length dependence

End effects are important for shorter rods. Global effects, such as rod length become more important for longer rods. We show in this section the range of lengths where end effects should be considered. For example, rods with concave ends show very similar response, independent of the inner radius D of the cavity when the rod is 200 nm long. The strength and position of the response depends sensitively on D when the rod is 100 nm long. In Fig. 6, we plot the far-field intensity for rods of different lengths when the rod has two hemispherical ends (HH) or one hemispherical and one concave end (CH). We considered a rod with a concave end because this termination gives the most effect. For rods longer than 100 nm, the resonances become increasingly similar and the end effects are much less important. For rods shorter than 100 nm, resonance position and, especially, the width depend on the termination. The short wavelength turn on shows up at similar wavelengths for the different terminations, but the long wavelength turn on is strongly blueshifted for the concave termination, reflecting the sharper resonance of the local oscillation.

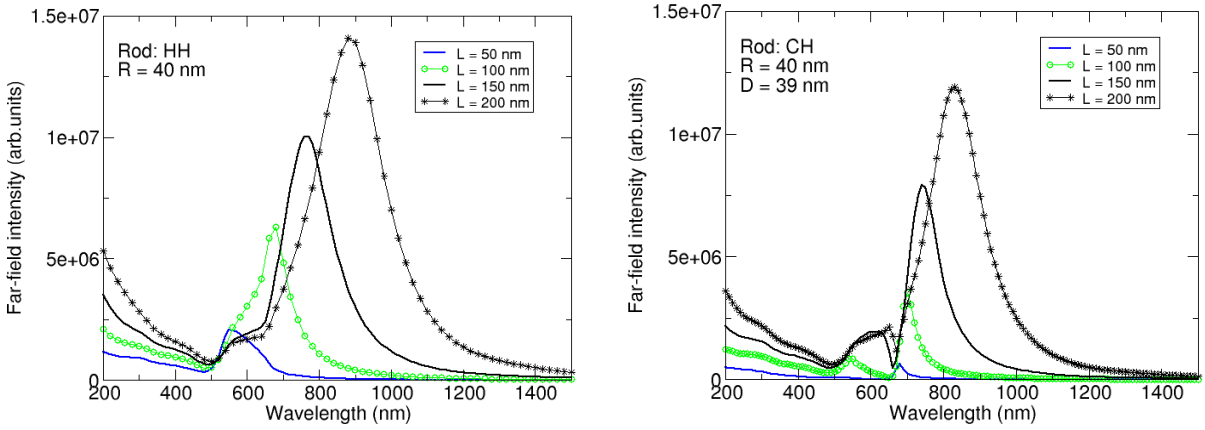

Fig. 6. (Left) Far field spectra for rods of different length having hemispherical terminations. (Right) Far field distribution of a rod of different lengths having one hemispherical end and one concave end.

5. SIZE DEPENDENCE

In antenna theory, the width of a conducting wire acting as a receiver or transmitter of radiation is usually considered to be very small compared to the length of the antenna. In the visible region, nanorods can have widths comparable to their lengths. Thus, tuning the transverse dimension provides another way to control the near and far field.. In Fig. 7, we plot the position of the resonances in single and coupled gold nanorods as a function of the rod width. We can clearly distinguish between two tendencies in the resonances positions. For rods with radii smaller than 30 nm, the resonances redshifts as the size decreases, as expected when the aspect ration (L/R) increases. For nanorods of length L=200nm, and radii larger than 30 nm, the resonances red shift as the width of the rods increases because retardation effects across the rod width become increasingly important. This provides a size regime for radii from 20 nm up to 40 nm where the resonance remains quite stable (see top of Fig. 7).

The effect of the width of the nanorod on the far field intensity and near field enhancement is also displayed in Fig. 7. The far field intensity increases when the rod width increases due to the presence of a larger dipole on the rods. This happens both for single rods and double rods. On the other hand, the near-field enhancement, (right) decreases as the radius increases due to the reduced charge density at a larger end. A larger radius provides a smaller lighting rod effect, and therefore a smaller near field.

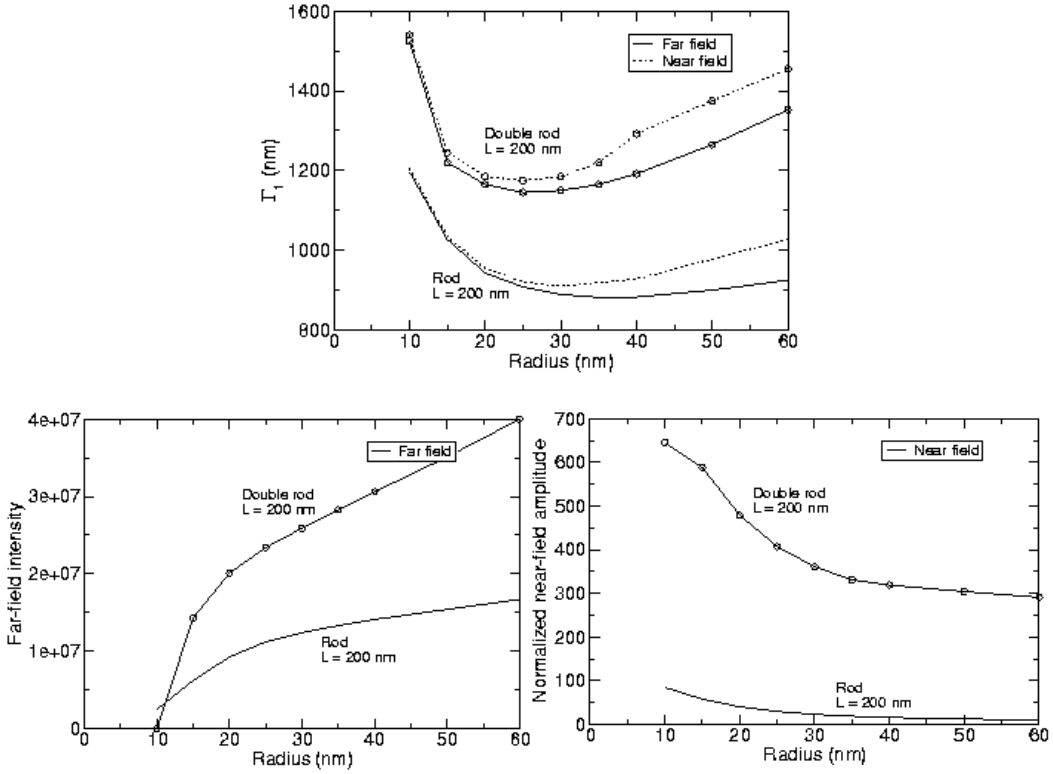

Fig. 7. (Top) Resonance positions Γ, as a function of rod radius for the far field and near field of 200 nm long single nanorods and double rods. (Bottom, left) Far-field intensity for light polarized along the rod axis, as a function of rod radius. (Bottom, right) Near field enhancement near the end of a 200 nm single rod and in the cavity of a double rod.

6. CONCLUSIONS

The resonances of gold nanorods depend strongly on conformational features of the rods. Single rods present resonances which depart from antenna theory due to the finite conductivity of gold at visible and infrared frequencies. We have shown in this paper how coupled gold nanorods have qualitatively different near- and far-field response when the rods are located at different separation distances. The effect of the termination of the rods is most important for short rods. For long rods, the main spectral peaks are well explained for rods with hemispherical and flat ends, as well as for rods with concave ends, in terms of dipolar excitations of the whole rod. For short rods with concave ends, the local charge oscillations inside the concave end and near the end on the outside of the rod determine the response. Finally, the thickness of the rods is an important control for tuning the response of the nanorod. Red shifts of resonances due to retardation in thicker rods and due to reduced charge accumulation at the ends of thinner rods both can be exploited to tailor the optical response of nanorods.

ACKNOWLEDGEMENTS

One of the authors (J.A.) acknowledges the "Gipuzkoa Fellows" program of the Diputación de Gipuzkoa, and the project ETORTEK-NANOTRON of the Basque Government.

REFERENCES

1. P. Mühlschlegel, H. J. Eisler, O. J. F. Martin, B. Hecht, D. W. Pohl, "Resonant Optical Antennas", *Science* 308 (2005).
2. A. J. Miller, S. W. Nam, J. M. Martinis, A. V. Sergienko, "Demonstration of a low-noise near-infrared photon counter with multi-photon discrimination", *App. Phys. Lett.* 83, 791 (2003).
3. J. Lee, J. P. Dulka, A. O. Govorov, N. A. Kotov, "Bioconjugates of CdTe Nanowires and Au Nanoparticles", *Nanoletters* 4, 2323 (2004).
4. C. Loo, A. Lowery, N. J. Halas, J. West, R. Drezek, "Inmunotargeted nanoshells for integrated cancer imaging and therapy", *Nanoletters* 5, 709 (2005).
5. A. Cvitkovic, N. Ocelic, J. Aizpurua, R. Guckenberger, R. Hillenbrand, "Infrared imaging of single nanoparticles via strong field enhancement in a scanning nanogap", *Phys. Rev. Lett.* 97, 060801 (2006).
6. S. A. Maier, P. G. Kik, H. A. Atwater, S. Meltzer, E. Harel, B. E. Koel, A.A.G. Requicha, "Local detection of electromagnetic energy transport below the diffraction limit in metal nanoparticle plasmon waveguides", *Nature materials*, 2, 229 (2003).
7. H. X. Xu, J. Aizpurua, S. P. Apell, M. Käll, "Electromagnetic contributions to single-molecule sensitivity in surface-enahnced Raman scattering", *Phys. Rev. E* 62, 2065 (2000).
8. T. Atay, J. H. Song, A. V. Nurmikko, "Strongly interacting plasmon nanoparticle pairs: from dipole-dipole interaction to conductively coupled regime", *Nanoletters* 4, 1627 (2004).
9. J. Aizpurua, P. Hanarp, D. S. Sutherland, M. Käll, Garnett W. Bryant, and F. J. García de Abajo, "Optical properties of gold nanorings," *Phys. Rev. Lett*. 90, 057401 (2003).
10. J. Aizpurua, Garnett W. Bryant, Lee J. Richter, F. Javier García de Abajo, Brian K. Kelley, and T. Mallouk, "Optical properties of coupled metallic rods for field-enhanced spectroscopy", *Phys. Rev. B* 71, 235420, (2005).
11. A. Hohenau, J. R. Krenn, G. Schider, H. Ditlbacher, A. Leitner, F. R. Aussenegg, W.L. Schaich, „Optical near-field of multipolar plasmonsof rod-shaped gold nanoparticles", *Europhys. Lett*. 69, 538 (2005).
12. J. B. Jackson, S. L. Wescott, L. R. Hirsch, J.L. West, N. J. Halas, "Controlling the surface enhanced Raman effect via the nanoshell geometry", *App. Phys. Lett.* 82, 257 (2003).
13. E. Prodan, C. Radloff, N. J. Halas, P. Nordlander, "A Hybridization model for the plasmon response of complex nanostructures", *Science* 302, 419 (2003).

14. F. Neubrech, T. Kolb, R. Lovrincic, G. Fahsold, A. Pucci, J. Aizpurua, T.W. Cornelius, M. E. Toimil-Molares, R. Neumann, S. Karim, "Resonances of individual metallic nanowires in the infrared", (to be published).
15. F. J. García de Abajo, and J. Aizpurua, "Numerical simulations of electron energy loss near inhomogeneous dielectrics", *Phys. Rev. B* 56, 15873 (1997)
16. F. J. García de Abajo, and A. Howie, "Relativistic electron energy loss and electron-induced photon emission in inhomogeneous dielectrics", *Phys.Rev. Lett.* 80, 5180 (1998).
17. F. J. García de Abajo, and A. Howie, "Retarded field calculation of electron energy loss in inhomogeneous dielectrics", *Phys. Rev. B* 65, 115418 (2002).